PROFILES OF INFRARED IRRADIANCE AND COOLING THROUGH A JET STREAM

DONALD R. JOHNSON
Department of Meteorology, University of Wisconsin, Madison, Wis.
WILLIAM C. SHEN*
Control Data Corporation, Minneapolis, Minn.

ABSTRACT

Vertical atmospheric cross sections of upward, downward, and net infrared irradiance, infrared cooling, temperature, potential temperature, and water vapor through a jet stream have been constructed for Jan. 7 and 9, 1961, along a line from International Falls, Minn., to Willemstad, Curacao. The profiles of irradiance and infrared cooling determined from filtered radiometersonde measurements clearly portray the influence of clouds. Variations of infrared irradiance and cooling associated with the zonal, secondary, and convective scales are discussed. Primarily attention is focused on radiation features associated with the jet stream and its associated cloud distribution. The contrast between profiles of net irradiance and infrared cooling between clear and cloudy regions is clearly portrayed. The range of infrared heating at the base of the clouds to the cooling at the top of the clouds exceeds 5–7°C./day. Apppreciable variations of infrared cooling are found in the stratosphere indicating the presence of water vapor, dust, tenuous cirrus, or other attenuating particles. The data indicate that a major factor controlling the horizontal variations of stratospheric infrared cooling is the high level cloudiness. The presence or absence of high level clouds primarily controls the source of infrared energy emitted from the earth and the troposphere, i.e., the upward irradiance which is available for stratospheric absorption.

1. INTRODUCTION

Of the diabatic processes occurring in the earth-atmosphere system, infrared emission alone serves to discharge the thermal energy. A question of considerable significance is whether infrared emission is important in determining the various modes of the atmosphere's circulation, or is merely a passive physical process to extract heat from the system. Presently the question is unanswered. However, from certain physical considerations, it is known that its dynamic importance is a function of scale size. With the recent addition of satellite radiation information, added impetus in the search for the determination of the importance of infrared processes is occurring. However, observational studies using satellite irradiance information can only describe the horizontal variation of the various components of irradiance at the atmosphere's fringe (Winston and Rao [17]; Allison, Gray and Warnecke [1]; Astling and Horn [2]) even though vertically the atmosphere is a highly non-isotropic radiator.

The purpose of this study is threefold: 1) to present a synoptic description of the vertical distribution of infrared irradiance to emphasize its non-isotropic structure, 2) to aid in the interpretation of the satellite's vertically integrated irradiance observations, and 3) to elaborate further on the irradiance processes associated with different scales (Kuhn and Suomi [7]). Primary attention is given to the infrared processes associated with the jet stream. However, the infrared structure of larger and smaller scales is evident from the analyses. The sparsity of radiometersonde data in time and space allows only tentative statements concerning infrared processes and the scales of motion. Still, we are satisfied that the analyses portray many interesting features that are important and that radiometersonde data supplementing satellite irradiance data on a synoptic scale would be valuable for both research and operational purposes.

2. ANALYSES AND DATA

Vertical cross sections portraying the fields of upward, downward and net infrared irradiance and the instantaneous infrared cooling, as well as the temperature, potential temperature, water vapor, and wind fields are prepared along a line from the northernmost station, International Falls, Minn., to the southernmost, Willemstad, Curacao. The data for the vertical cross sections were provided by radiometersonde flights at International Falls, Minn., Peoria, Ill., Nashville, Tenn., Montgomery, Ala., Grand Cayman Island, and Willemstad, Curacao, at the regularly scheduled synoptic times of 0000 GMT, Jan. 7 and 9, 1961. Supplementary 0000 GMT data were provided by the radiosonde flights at Green Bay, Wis., and Tampa, Fla. Filtered estimates of the irradiance components and infrared cooling were determined from radiometersonde data using the polynomial filtering technique described by Kuhn and Johnson [6]. The frequency response of this

*The research presented in this paper was conducted while the author was a member of the Department of Meteorology at the University of Wisconsin.

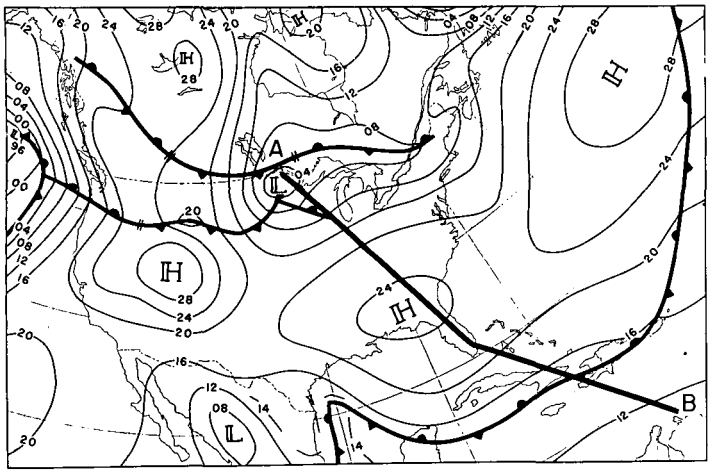

FIGURE 1.—Surface chart, 0000 GMT, Jan. 7, 1961. Solid line from A to B is the position of the vertical cross section.

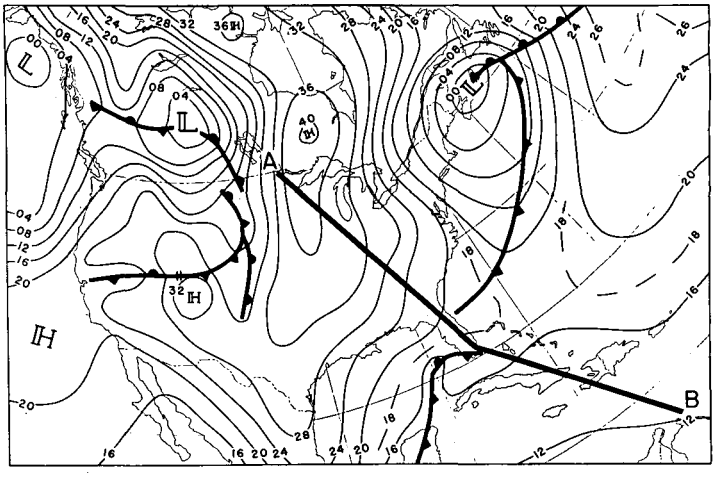

FIGURE 2.—Surface chart, 0000 GMT, Jan. 9, 1961. Solid line from A to B is the position of the vertical cross section.

polynomial filtering technique for the radiometersonde data is 0.23 for a vertical wavelength of 0.8 km., 0.65 for 1 km., and 0.92 for 1.6 km.

Surface and constant pressure charts based on analyses from the National Meteorological Center are presented with slight modifications in figures 1 through 3. Since our purpose is to discuss several characteristic features of the irradiance field, synoptic considerations are limited to a brief discussion of the broad-scale circulation features of Jan. 7 and 9, 1961.

3. SYNOPTIC DISCUSSION

On the 0000 GMT surface chart for January 7 (fig. 1), the predominant surface features are the high pressure area located in the southeastern United States and a developing low pressure area in northern Minnesota. The high pressure area centered in Georgia was of maritime polar origin, having migrated from the Pacific across the southwestern United States. Since the High was slowly weakening, the developing low pressure area was the dominant surface feature by Jan. 8, 1961. By January 9 the Minnesota low pressure area moved eastward to the Nova Scotia peninsula and deepened from a central pressure of 1002 mb. on the 7th to 998 mb. on the 9th (see fig. 2). The cold front trailed southwestward over the Atlantic Ocean to northern Florida with the extremely cold continental arctic (cA) air and the overlying, deep tropospheric, continental polar (cP) air having moved behind the cold front from the lee of the Canadian Rockies southeastward over the eastern half of the United States. The high pressure center of 1041 mb. remained in Canada and by virtue of its strength and position continued to feed cold air from Canada to the eastern United States. Another surface feature of interest was the weak stable wave in the Gulf of Mexico east of Brownsville, Tex. On January 7 the stationary portion of an old polar front extending from the central North

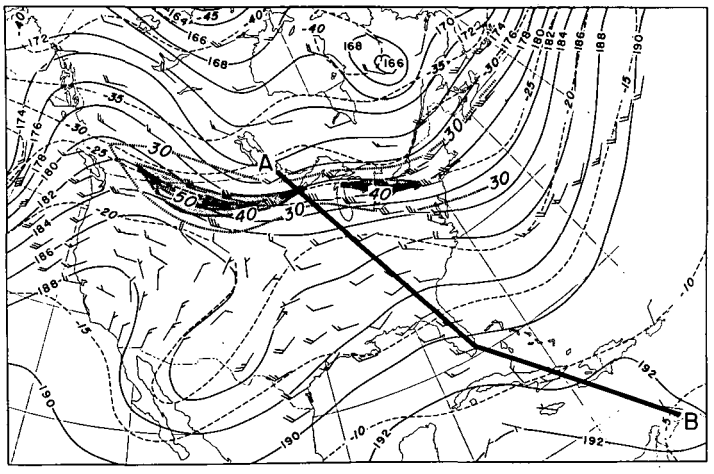

FIGURE 3.—500-mb. chart, 0000 GMT, Jan. 7, 1961. Solid line from A to B is the position of the vertical cross section.

Atlantic into the Gulf of Mexico was undergoing frontolysis, but since the stable wave had vertical continuity to the cutoff 500-mb. Low over western Texas (fig. 3), it maintained its identity.

At the 500-mb. level on January 7 (fig. 3), two distinct trajectories were embedded in the westerly flow over the eastern half of the United States. One trajectory from the west-northwest was associated with the polar jet which was located in the upper troposphere along the northern United States border above the north-south temperature contrast between the maritime polar (mP) air over the central United States and the colder cP air over Canada. The maximum speed of the jet was approximately 45 m./sec. at the 300-mb. level over Green Bay, Wis. In all analyses shaded regions indicate wind speeds greater than 40 m./sec.

Farther south the other trajectory was associated with the high tropospheric subtropical jet. The subtropical jet was situated above a weak baroclinic zone in the middle

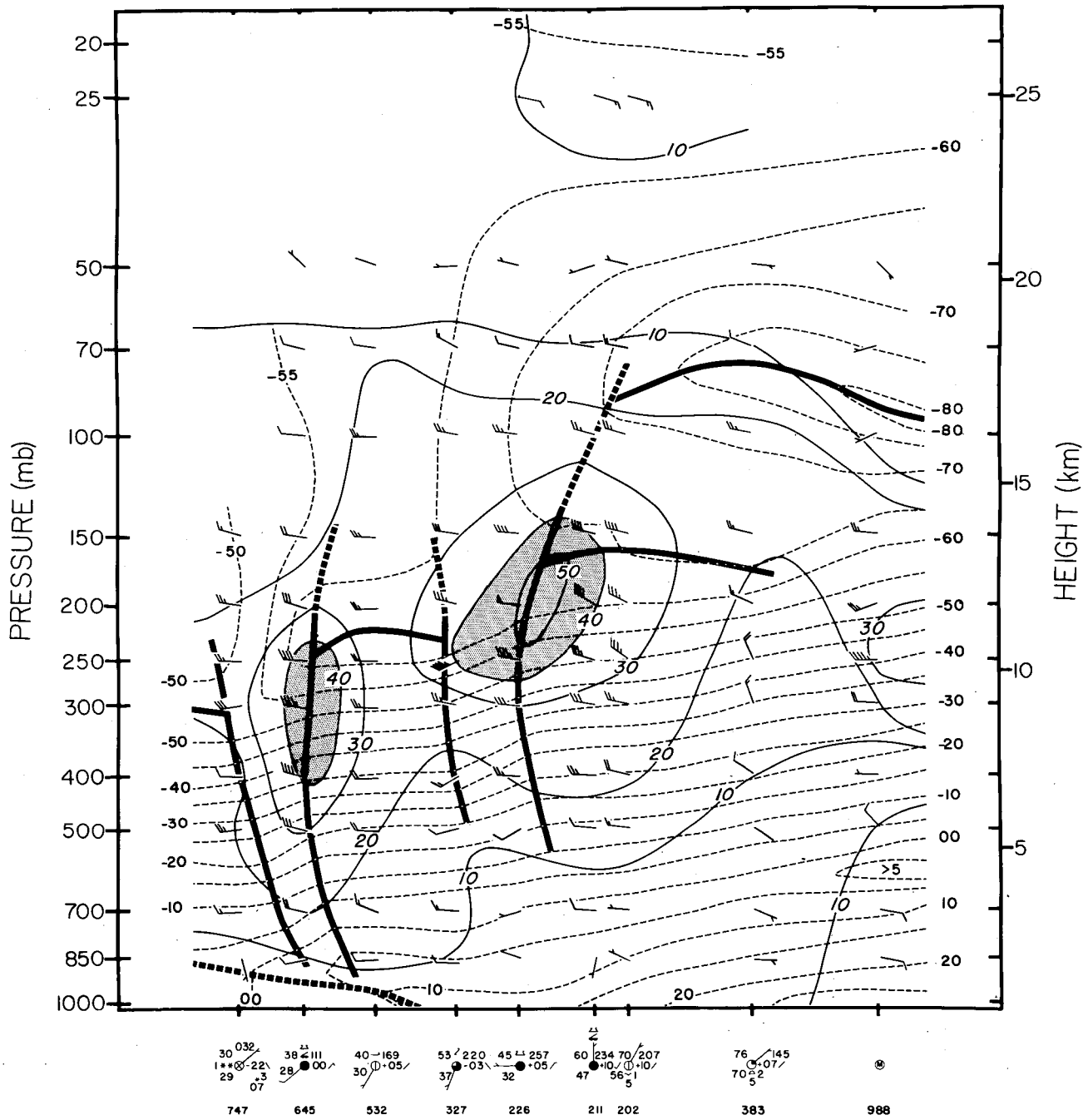

FIGURE 4.—Temperature (°C.) and wind (m./sec.) analysis, 0000 GMT, Jan. 7, 1961. In the plotted winds whole barbs indicate 10 m./sec., half barbs indicate 5 m./sec. Shaded regions delineate region of wind speeds greater than 40 m./sec. Heavy solid vertical lines indicate leading and rear boundaries of frontal zones with strong thermal support; dashed lines indicate frontal zones with weak thermal support. Heavy solid horizontal lines indicate tropopause.

and upper troposphere between the mP air over the central United States and the maritime subtropical (mT) air of the Caribbean. At 200 mb., the upper tropospheric jet extended along the Gulf and appeared as a broad band of moderate speeds with a maximum near 55 m./sec.

By the 9th, the two jets had merged into a broad band of maximum winds with a particularly complicated structure as the cold polar air of the upper troposphere moved over the eastern United States. The sequence of events during the 48-hr. period and pattern of the merged jets are similar to those described by Reiter [13]. The maximum wind speeds are located at the southern edge of the strongly developed cold upper level trough lying over the New England States. The subtropical portion of the merged jet at the 200-mb. surface on the 9th, had speeds in excess of 70 m./sec. as the frontal zones became juxtaposed and the baroclinicity of the polar front intensified.

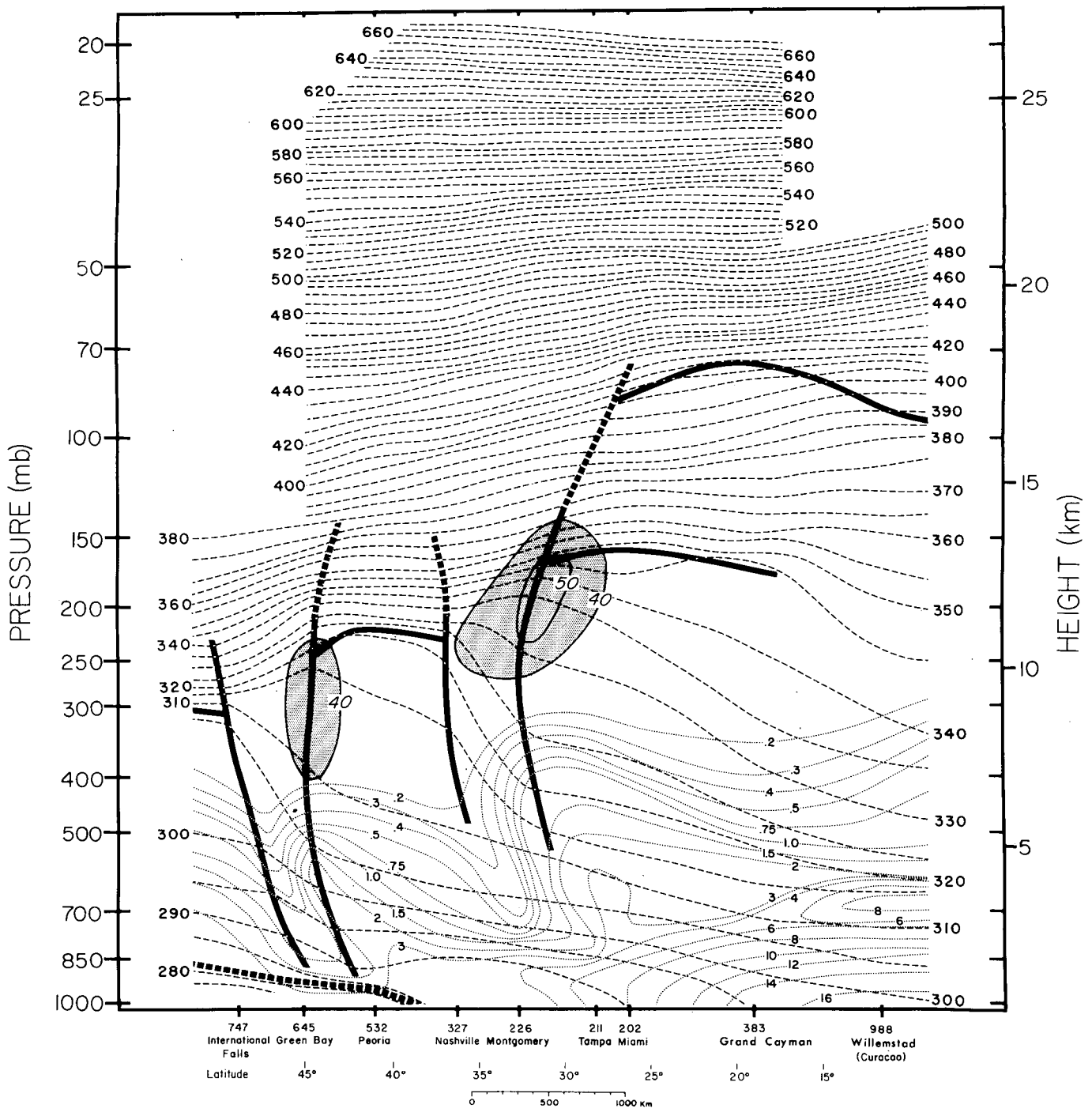

FIGURE 5.—Potential temperature (°K.) and water vapor (gm./kg.) analysis, Jan. 7, 1961. Heavy solid vertical lines indicate leading and rear boundaries of frontal zones with strong thermal support; dashed lines indicate frontal zones with weak thermal support. Heavy solid horizontal lines indicate tropopause.

4. TEMPERATURE, WIND, POTENTIAL TEMPERATURE, AND WATER VAPOR ANALYSES

The 0000 GMT cross-sectional analyses of the temperature and wind field for January 7 and 9, are presented in figures 4 and 6 while the corresponding analyses of potential temperature and water vapor are presented in figures 5 and 7. The 0000 GMT surface observations and station locator numbers are shown at the base of figures 4 and 6. The station names, locator numbers, latitude, and scale are shown on all other cross sections as well as the maximum wind regions to be able to locate pertinent features with respect to the jet's position.

The heavy dashed line on the cross sections for the 7th indicates the upper boundary of a bubble of very shallow modified cA air associated with a previous arctic outbreak. The polar frontal zone over Green Bay, Wis., separates the extremely cold shallow cA and deep tropo-

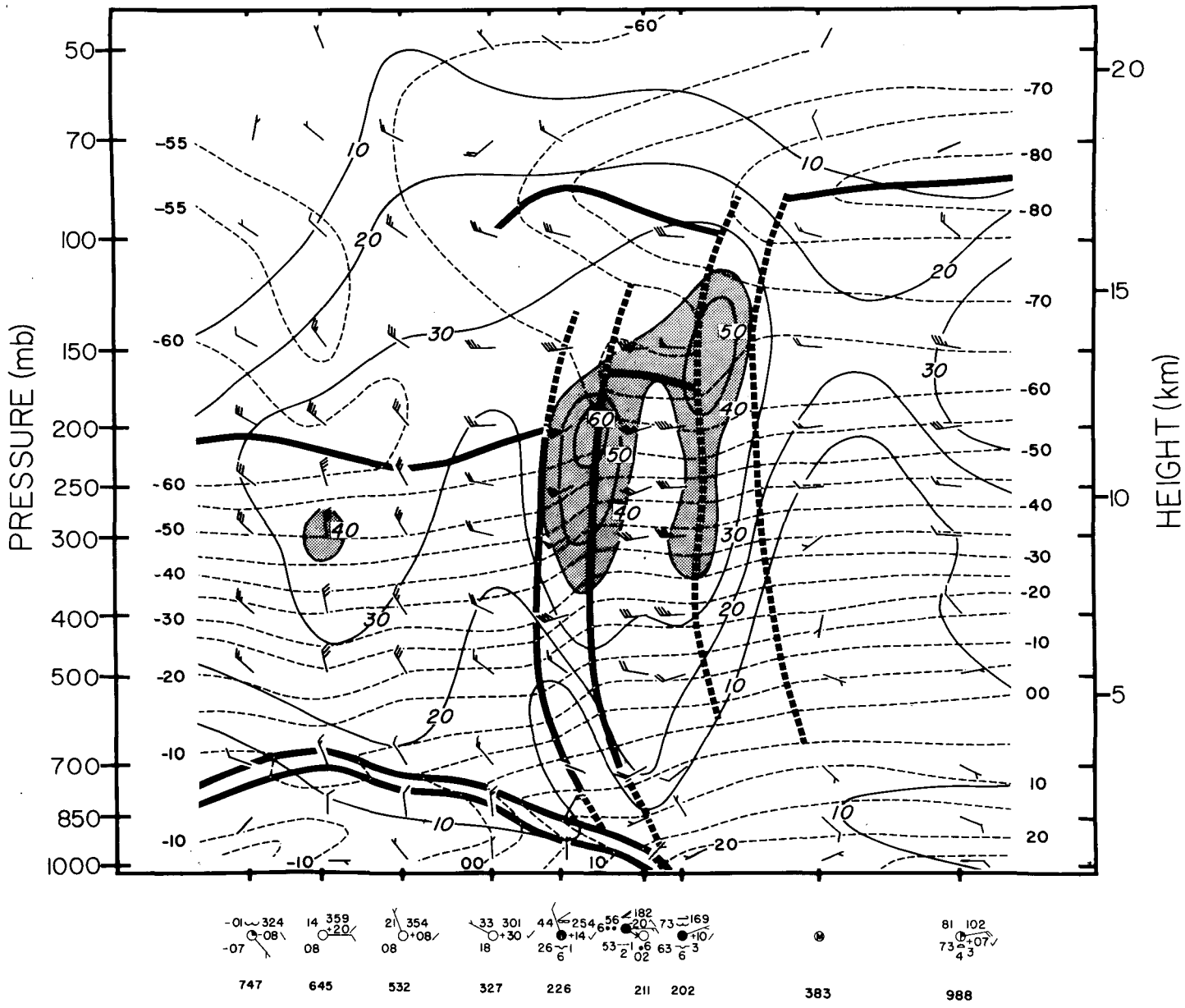

FIGURE 6.—Temperature (°C.) and wind (m./sec.) analysis, 0000 GMT, Jan. 9, 1961. For explanation, see caption of figure 4.

spheric cP air to the north from the modified mP air over the central United States. As noted before, the temperature contrast between mP air over the United States and the mT air over the Caribbean lies in the upper troposphere and is clearly shown in figures 4 and 5. The lower of the two tropopauses in the Caribbean area is the subtropical tropopause over the mT air while the higher must be an extension from the low latitudes of the very high tropical tropopause.

The rising warmer moist air south of the two frontal zones on the 7th and of the polar front on the 9th is clearly delineated from the subsiding drier air to the north by the water vapor analysis. The observations for Green Bay, Wis., and Montgomery, Ala., on the 7th and Montgomery on the 9th indicated increasing moisture with height as the radiosonde ascended through the frontal zones. Thus, the maximum horizontal gradient of the moisture field was positioned in the frontal zones. The water vapor contrast across the front, indicating the opposing vertical motion, is likely evidence of a thermally direct vertical circulation of the type proposed by Eliassen [5]. From quasi-geostrophic theory Eliassen notes that a transverse circulation of the direct type should exist for tropospheric cold fronts.

At the base of figure 4 the surface weather conditions on the 7th indicate a region of extensive cloudiness north of Green Bay associated with the developing unstable wave. The other area of extensive cloudiness from Nashville, Tenn., to Tampa, Fla., was associated with the subtropical jet. Generally fair weather conditions existed from just

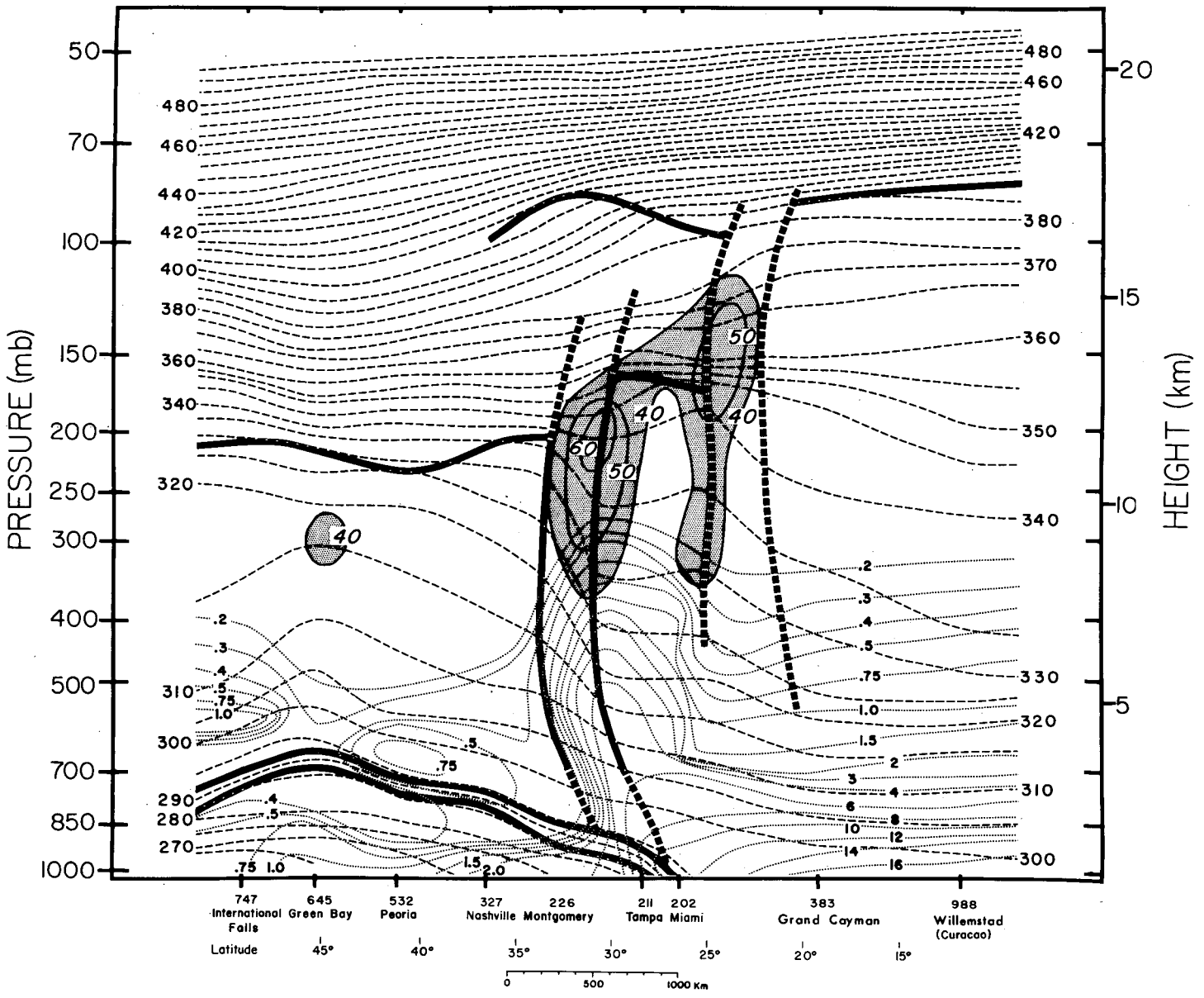

FIGURE 7.—Potential temperature (°K.) and water vapor (gm./kg.) analysis, 0000 GMT, Jan. 9, 1961. For explanation, see caption of figure 5.

south of Green Bay to Nashville and to the south of Tampa. The cloudy and precipitating regions are emphasized since these conditions greatly attenuate the components of infrared irradiance.

In figure 6 the weather conditions for the 9th indicate that the region of extensive cloudiness was confined to the southern United States. The cloudiness was associated with the trailing polar front and the stable wave off the western Florida coast (see fig. 2).

5. UPWARD, DOWNWARD, AND NET IRRADIANCE PROFILES

The profiles of the upward, downward, and net irradiance (ly./min.) for Jan. 7, 1961, are portrayed in figures 8 through 10. Profiles for the 8th and 9th were prepared to study the continuity of the irradiance fields. However, the results are not presented since the time continuity is excellent and they display similar processes. The principal variation in the cross sections of upward and downward irradiance occurs in the vertical with the magnitude of the components of irradiance decreasing from the earth's surface upwards. The well-known decrease in the upward directed irradiance is explained by the absorption of a portion of the earth's black body radiation by the intervening constituents of water vapor, carbon dioxide, ozone, particulates, and sometimes clouds and reemission of a portion of the absorbed energy at a lower temperature. Exceptions to the general decrease upwards occur within clouds and the stratosphere where the upward flux is relatively constant. In the stratosphere the upward flux occasionally increases after the balloon ascends through an upper cloud boundary that lies near the tropopause.

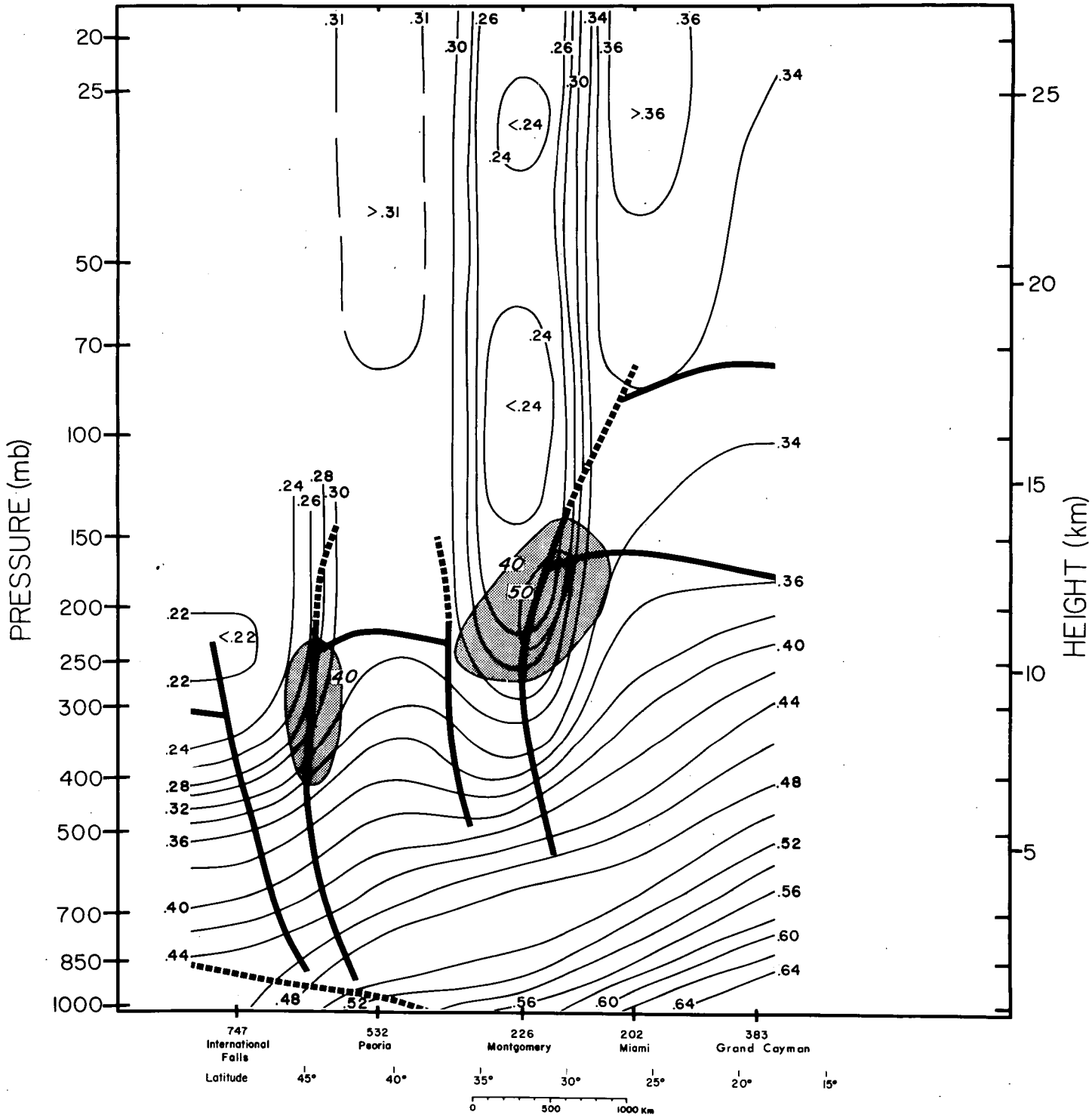

FIGURE 8.—Upward irradiance (ly./min.) analysis, 0000 GMT, Jan. 7, 1961. See caption of figure 5 for explanation of frontal boundaries and tropopause.

The increase of upward irradiance in the stratosphere is due to the increased radiant energy being emitted from stratospheric regions with higher temperatures than the cloud top temperature.

The magnitude of the downward irradiance always decreases with height unless a layer effectively acting as a black body lies higher in the atmosphere. Such conditions are associated with cloud layers embedded within inversions or an isothermal layer within which the density of absorbing constituents increases with height. The latter condition is indicated for the tropical stratosphere in figure 9. The magnitude of the change is so small that the event can be explained as a presence of random instrumental errors. However, in this example and other data

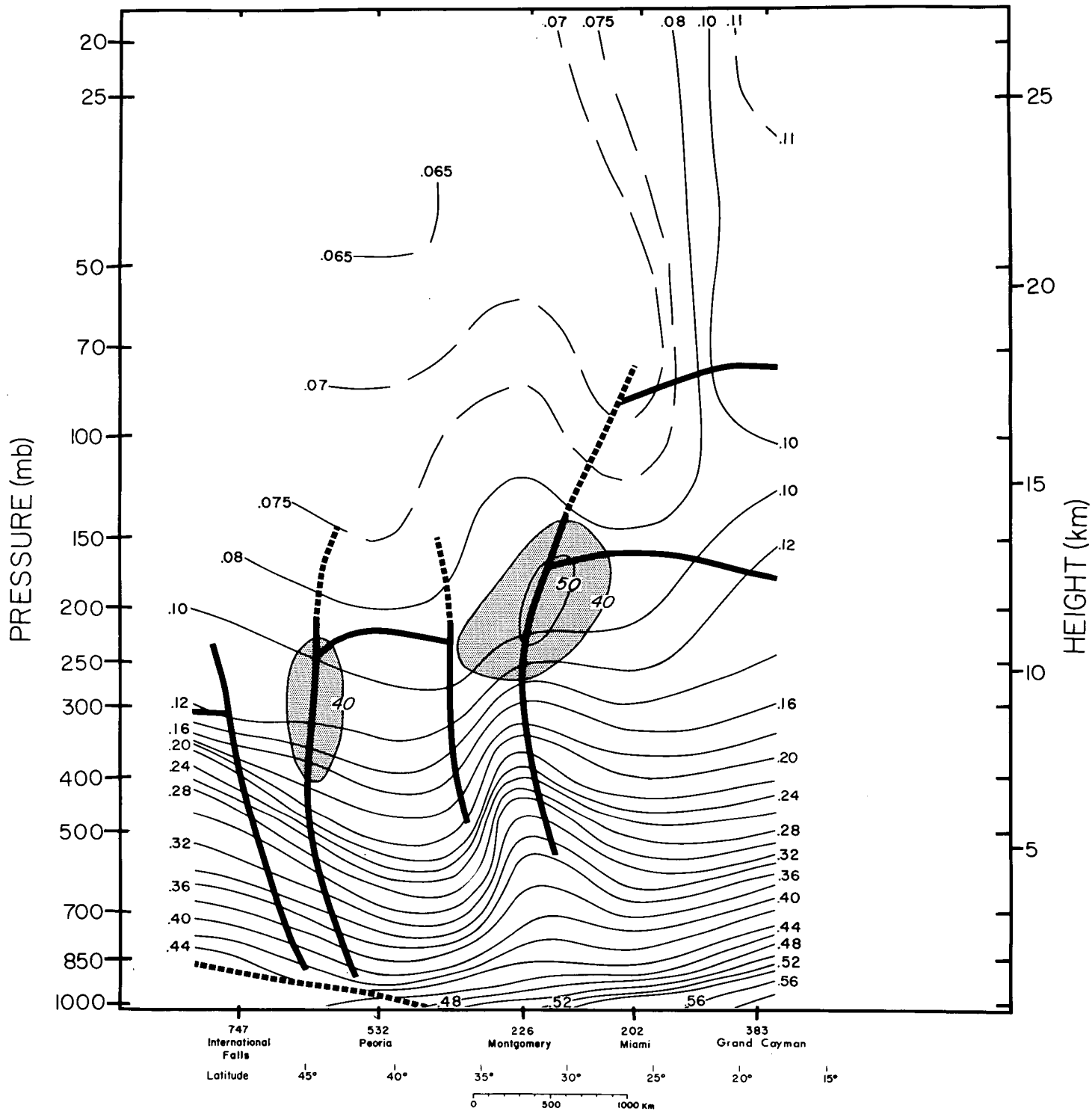

FIGURE 9.—Downward irradiance (ly./min.) analysis, 0000 GMT, Jan. 7, 1961. See caption of figure 5 for explanation of frontal boundaries and tropopause.

there were changes in both the upward and downward irradiance which indicate significant and unexplained variations of stratospheric dust, water vapor, or possibly tenuous cirrus clouds.

In contrast to the decrease of upward and downward irradiance with height, the net irradiance usually increases with height (see fig. 10). This is because the rate of decrease with height of downward irradiance is greater than that for the upward component. Exceptions to this condition occur in the vicinity of clouds.

The variation in the irradiance components associated with the largest scale, the hemispheric scale, is usually a poleward decrease at all elevations of the upward, downward, and net irradiance. The variation of the upward

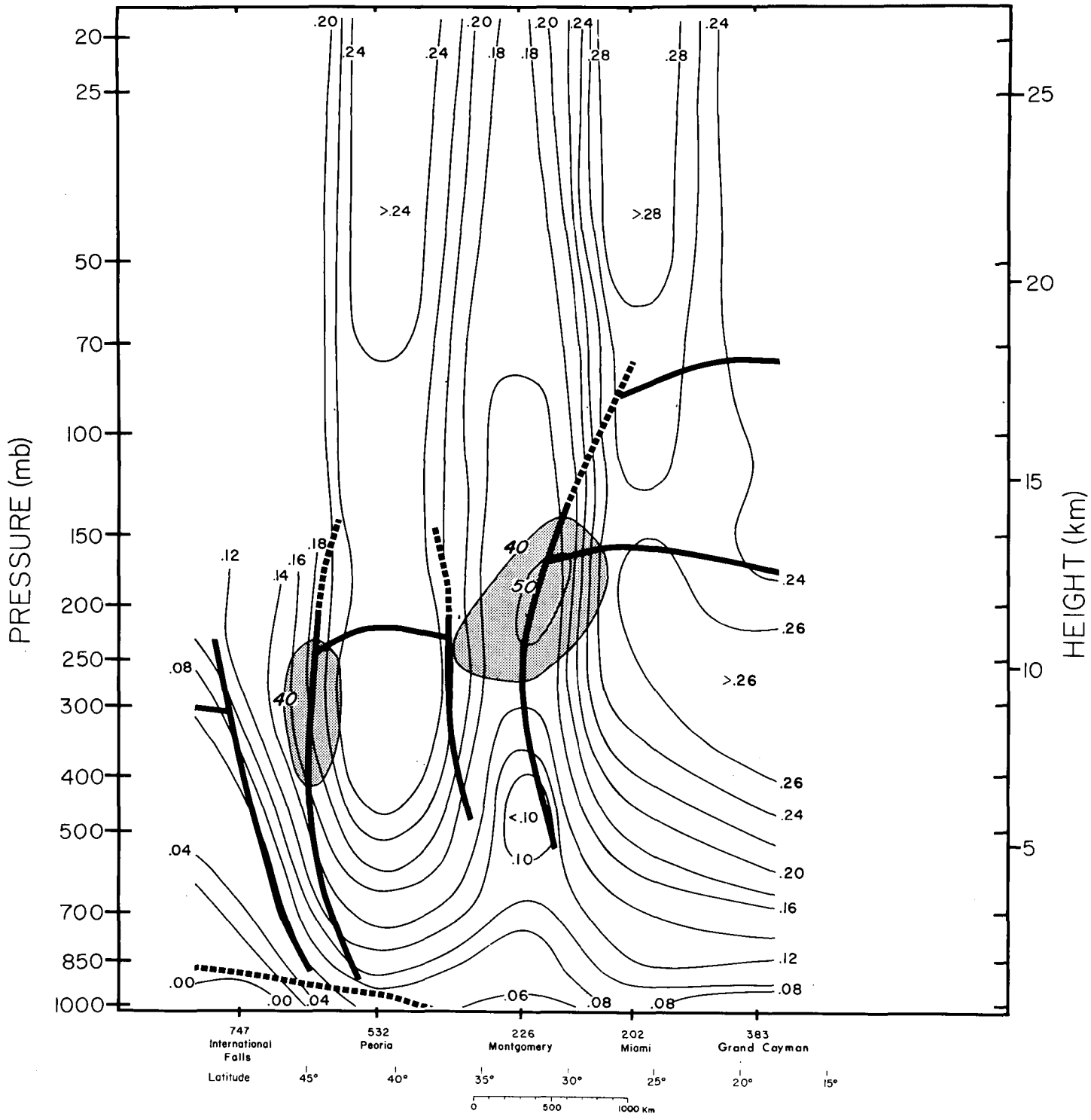

FIGURE 10.—Net irradiance (ly./min.) analysis, 0000 GMT, Jan. 7, 1961. See caption of figure 5 for explanation of frontal boundaries and tropopause.

directed irradiance is due to the decreasing infrared emission associated with the lower surface and tropospheric temperatures as one moves northward. The decrease of the downward irradiance must be solely attributed to the lower tropospheric temperatures of the polar latitudes since the upward facing radiometer never views the earth's surface.

The effect of clouds may modify the gentle poleward decrease of the downward directed irradiance as shown in figure 9. On the 7th the downward directed irradiance over International Falls, Minn., in the middle and upper troposphere was nearly equal to that over Grand Cayman Island due to the intensive cloudiness associated with the developing wave over the northern United States. The

cold polar tropospheric clouds effectively behaving as black bodies emit nearly as much downward directed energy as the warmer clearer subtropical troposphere.

The next largest scale with its more striking influence is the variation of infrared irradiance associated with the organized cloud structure of the jet stream and the frontal zones. In figure 8 the upward irradiance in the cloudy regions is less than in the clear troposphere. Note the relative minima on the horizontal surfaces which intersect the cloudy regions of the subtropical jet stream and the upper level baroclinic zone. The downward facing radiometer will always receive less energy when it is in or above a cloudy region than when it is above a clear region with an equal surface temperature. In the cloudy region the radiometer receives the infrared energy emitted by the cloud's colder black body surface while in the clear region it receives energy from the earth's warmer black body surface which is only somewhat attenuated by the intervening absorbing constituents.

In figure 9 for the downward irradiance relative maxima in the horizontal direction occur in and beneath the cloudy regions of the jet stream and the frontal zones. The upward facing radiometer in and beneath clouds receives more energy from the clouds due to their effective black body behavior than if it were at an equivalent pressure surface with a clear overlying atmosphere. The greatest contrasts for the horizontal variation of downward irradiance occur in the high troposphere and are depicted in the irradiance cross sections above Montgomery, Ala., on the 7th.

The effects of high and middle clouds are even more striking in the profiles of net irradiance in figure 10. On the 7th in the free atmosphere the minimum values of net irradiance on a horizontal surface occurred within the multilayer cloud structure over Montgomery, Ala., and International Falls, Minn. Note that snow was falling at International Falls. The effect of organized middle- and high-level clouds on the upward irradiance near the top of the atmosphere for this scale of motion is clearly portrayed by the magnitude of the upward irradiance at the top of figure 8. At the 150-mb. level a minimum value of approximately 0.24 ly./min. of upward irradiance is indicated over the subtropical jet while a maximum value of 0.35 ly./min. is indicated for the subtropical Caribbean; these are representative values that are observed by the satellite infrared sensors.

6. INFRARED COMPONENT OF ATMOSPHERIC HEATING

As noted in the introduction, the sole component of diabatic heating that serves to discharge thermal energy from the earth-atmosphere system is that due to infrared emission. Lorenz [9] and others have considered the problem of explaining why the intensity of the atmosphere's circulation is so low in comparison to the total energy received and emitted by the atmosphere. Our purpose is not to explore this question but to note that the role of infrared emission is a fundamental consideration in the answer to this problem. From classical thermodynamic considerations, the efficiency of the "thermodynamic engine" in producing mechanical energy not only depends on the temperature at which the heat is added but also on the temperature at which it is extracted. The coupling process for the thermal energy source and sink which produces the mechanical energy is the adiabatic expansion phase. These fundamental thermodynamic considerations were emphasized by Mintz [10] and the importance of these considerations in the generation of available potential energy for the atmosphere's circulation is evident in the results of Dutton and Johnson [4]. From the concept of available potential energy as a basis for their diagnostics, they obtained a generation due to the infrared component of 1.61 watts/m.^{2}, which was 29 percent of the total generation of zonal available potential energy. The large positive value is due to the efficiency of the generation process in the cold polar troposphere coupled with the significant infrared emission from that portion of the atmosphere.

At scales of atmospheric motion intermediate to the zonal and the cloud convection scale the importance of infrared cooling is largely undetermined. However, the cross sections of instantaneous infrared cooling due to the infrared divergence for both January 7 and 9 are presented to gain some insight into representative values for the large planetary, secondary, and convective scales of the atmosphere.

In the cross section of infrared cooling for the 7th and 9th (fig. 11 and 12) the dominant patterns are due to the effects of clouds. To a lesser degree there is a hemispheric scale associated with the poleward decrease of temperature, for on the 9th the mean cooling of the subtropical region is approximately 1.7°C./day, while it is near 1.0° C./day in the polar region.

The effects of clouds on the 9th is evidenced by the heating of 3°C./day at the base of the middle cloud and the cooling of 4 to 5°C./day at the top of the multilayered clouds over Miami. Undoubtedly this vertical variation of the infrared component of diabatic heating is important in determining the structure and intensity of the ascending and decending motions within the cloud by which latent heat is released and both water vapor and sensible heat are redistributed through the cloud destabilization process. The rate of destabilization is greater, the higher the cloud (Möller [11]) and the larger its effective emissivity. In addition the process is enhanced when the clouds are above warm surfaces as over Florida and the tops reach the high troposphere so there is little back radiation from the overlying atmospheric mass to offset the effective black body cooling of the cloud top. The destabilization process is also portrayed to a lesser extent by the profile of infrared cooling above International Falls, Minn., on the 7th. In this case, there is little heating at the cloud's base since the clouds are multilayered and

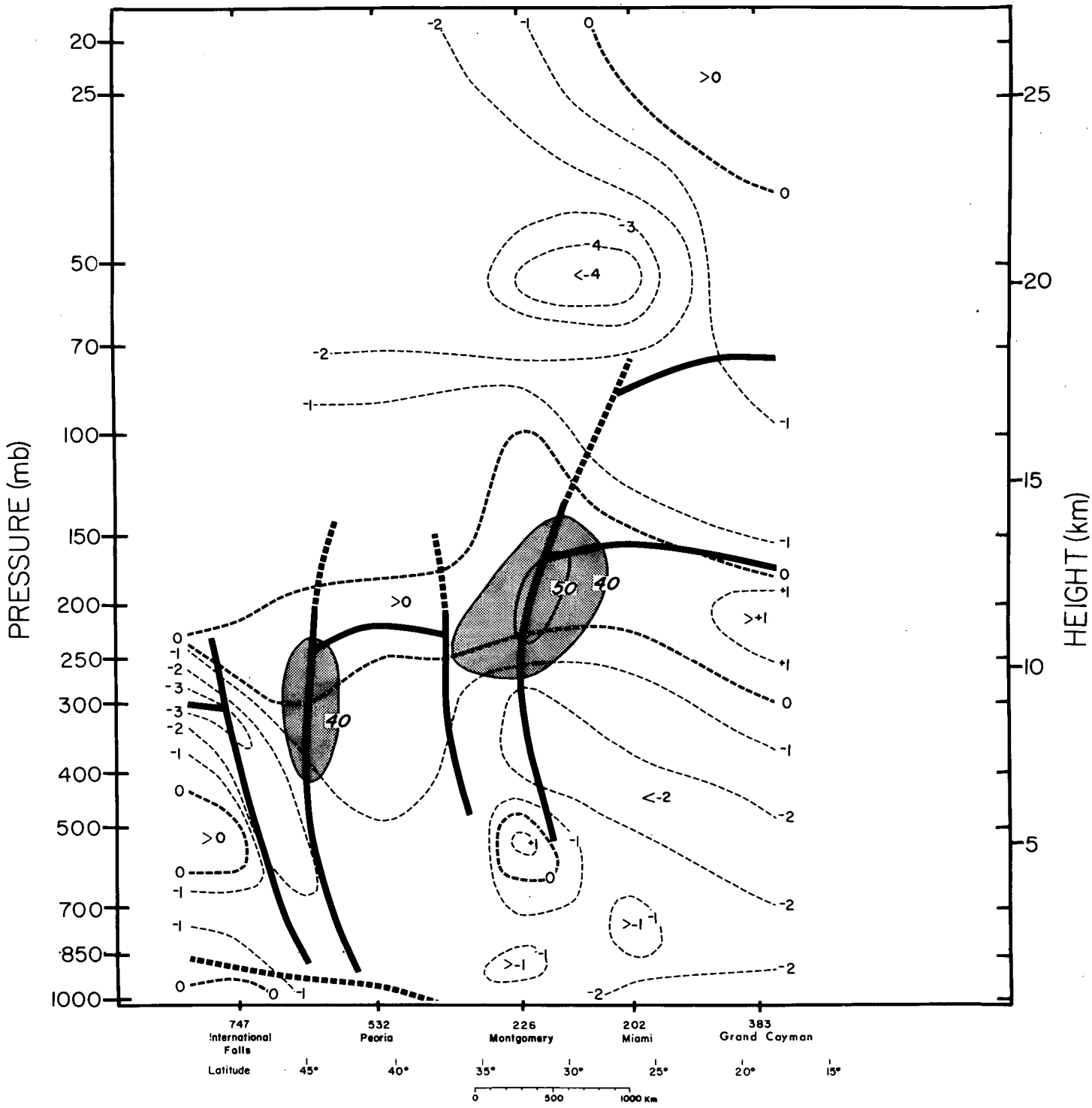

FIGURE 11.—Analysis of instantaneous atmospheric heating (°C./day) by net irradiance divergence, 0000 GMT, Jan. 7, 1961. See caption of figure 5 for explanation of frontal boundaries and tropopause.

over a snow-covered surface. Thus the difference in the upward impinging irradiance and the downward emitted irradiance at the cloud's base over International Falls was much less than at the middle cloud base above Miami on the 9th.

One interesting feature of the cooling profile on the 7th (fig. 11) is the small positive heating of 1.0°C./day near 550 mb. over Montgomery, Ala. The only cloud reported at 0000 GMT is a high overcast of cirrostratus. The first indication of lower clouds is an observation at 0340 GMT

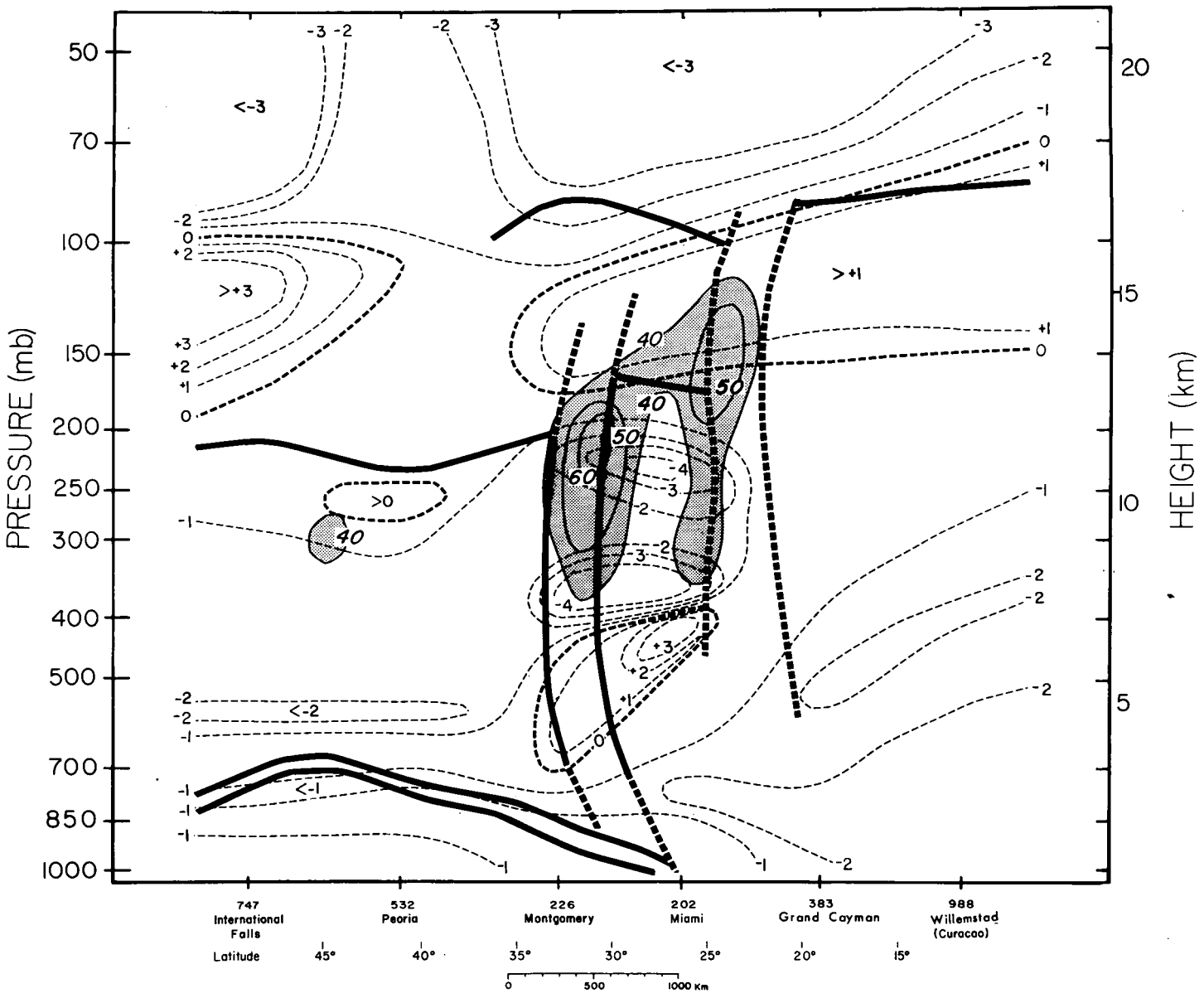

FIGURE 12.—Analysis of instantaneous atmospheric heating (°C./day) by net irradiance divergence, 0000 GMT, Jan. 9, 1961. See caption of figure 5 for explanation of frontal boundaries and tropopause.

of 8/10 coverage of altocumulus with an estimated base of 18,000 ft. The two possibilities are that either the observer missed the lower deck of clouds under the cirrostratus overcast in his nighttime observation at 0000 GMT or the radiometer was sensing the moisture contained in an isentropic layer that was being advected ahead of the visible cloud structure. The latter explanation seems preferable since the cirrostratus is reported to be a high overcast from before sunset to 0140 GMT, then broken between the 0140 GMT observation at the 0340 GMT observation. This indicates that the observer was able to estimate some characteristics of the cloud structure in his nightime observation, thus adding evidence to his observation of no reportable clouds below the high cirrostratus overcast.

In both figures 11 and 12 a slight heating of the region near the tropopause is indicated. On the 7th the heating rate is generally positive but less than 1°C./day. On the 9th higher heating rates are indicated although less clearly organized. These results agree with Darkow's [3] conclusion that the infrared component generally serves to heat the region of the tropopause.

One of the most interesting but speculative results of this study is the stratospheric field of infrared cooling on the 9th. On both the 7th and the 9th (fig. 11 and 12)

relatively intense cooling is indicated for the stratospheric region near 20 km. above the high clouds of the subtropical jet. The actual magnitude of the cooling may be questionable since the cooling estimates for the stratospheric region are less reliable than for tropospheric and the sounding at Miami terminated before reaching 50 mb. However, the data indicate that the cooling rates of the stratospheric regions above high tropospheric clouds tend to exceed the cooling rates above clear areas. This difference can be partially attributed to the fact that there is 30–50 percent less upward directed irradiance to be absorbed by the stratospheric mass over the high cloudy regions than over a clear area with a high surface temperature. Quite likely there must also be a higher concentration of the variable effective emitters, either particulates, ozone, water vapor, or ice crystals, to account for the increased loss of radiant energy in localized regions of the stratosphere.

Another interesting feature in figure 12 is the region of heating and cooling in the stratospheric air above International Falls, Minn., on the 9th. In the surface observation high thin cirrus is reported 1 hr. prior to 0000 GMT but at 0000 GMT only a layer of 2/10 altocumulus at 8,000 ft. is reported. The most likely explanation for the heating and cooling in the stratospheric regions is that tenuous cirrus actually exists in the stratosphere near 100 mb. On the surface chart for the 9th (fig. 2), a weak occluded system lies over the western Dakotas. The subtropical tropopause associated with this system is near 100 mb., thus indicating that the attenuating layer over International Falls near 100 mb. may be a tenuous layer of cirrus being advected isentropically ahead of the occluded system into the stratospheric regions over the cold polar air mass. This process associated with the secondary circulation scale serves to inject water vapor from the troposphere into the stratosphere and can be readily detected by radiometersonde observations.

7. RELATIONSHIP OF SATELLITE AND RADIOMETERSONDE IRRADIANCE OBSERVATIONS

Radiometersonde observations of upward irradiance high in the stratosphere above any organized attenuating layers are directly comparable with satellite infrared observations if certain geometrical relations are satisfied and both instruments possess similar spectral sensitivity. The horizontal variations of the absorbed and reemitted energy of the intervening mass between a radiometer high in the stratosphere and a satellite are extremely small in comparison to the magnitude range of both observational series.

Our immediate purpose in this discussion is to illustrate how satellite irradiance data contain information for locating jet streams if associated clouds patterns are present. Previous results indicate that both cloud photographs (Oliver, Anderson, and Ferguson [12]; Whitney, Timchalk, and Gray [15]) and satellite radiation data (Allison, Gray, and Warnecke [1]) are useful for locating the jet-stream axis. Whitney et al. present an excellent summary and discussion of the physical processes that produce characteristic cirrus shield with a sharply defined poleward edge. Although both location techniques primarily depend on the presence of a cirrus shield, the two techniques used jointly will provide greater reliability than each used separately. Our upward irradiance cross section (fig. 8) illustrates the effects of organized clouds in creating variations in the upward irradiance field of the stratosphere. Since the same cloud features will produce similar variations in the satellite observational series, the radiometersonde values at the top of the cross section can be considered representative of satellite data. Spectrally such a given hypothetical satellite series is comparable to TIROS II channel 4 observations of the 7–32-micron region of the terrestrial infrared spectrum [14].

Returning to figure 8 for the upward irradiance, and assuming that the values of the upward irradiance at the top of the cross section are representative of the satellite observations, one finds it apparent that the effect of clouds associated with the jet stream produce significant variations in the hypothetical satellite irradiance. In figure 8 the upward irradiance between the cloudy and clear regions of the subtropical Caribbean ranges from approximately 0.24 to 0.34 ly./min. These are representative values observed by the satellite experiments. Note that the maximum gradient is located at the equatorward edge of the jet stream which agrees with Winston's [16] result that the magnitudes of the westerlies and the gradient of upward irradiance observed by satellites are positively correlated. The effects of high clouds in producing variations in satellite observations will be the greatest when the contrast between the background upward irradiance of the earth's surface and the cloud top irradiance is greatest. Thus, the larger the difference in the equivalent black body temperatures of the two radiating surfaces, the better is the detection capability. Subtropical jets should be easier to detect than polar jets since the contrast in the upward irradiance emitted by the jet stream cirrus shield and the earth's tropical surface is greater than the corresponding contrast at higher latitudes. Furthermore the usually more dense subtropical cirrus shield lying higher in the troposphere will probably possess the lowest equivalent black body temperatures. The latter condition partially depends on the effective emissivity of the cloud layer (Kuhn and Suomi [8]). For a jet stream over a very cold surface, a cyclonic upper level cold core vortex with extensive clouds or any similar low-valued irradiance background region, the satellite irradiance location technique may fail to discriminate the jet stream location. Satellite data may also fail over jet cores that do not have high-level clouds to produce attenuation of the irradiance field. The satellite irradiance data would be particularly valuable when photographic techniques fail because the shadow cast on lower cloud surfaces or on the earth (Whitney et al. [15]) cannot be detected due to an unfavorable

geometric arrangement of the sun, earth, and satellite. Furthermore, at night, the irradiance data are the only satellite observations that can provide information on the detection of this important feature.

8. CONCLUDING REMARKS

While not emphasized, the fields of the irradiance components and infrared cooling were all determined from filtered radiometersonde data. From the detailed structure shown in the cross sections, it is clear that the use of filtering polynomials does not obscure the basic structure of the fields even in the vicinity of the cloud boundaries. Without filtering, it is not possible to determine the detailed structure of the infrared cooling profiles due to the dominating effects of the random error component.

In conclusion we simply note that our threefold purpose presented in the introduction was fulfilled. The results presented are tentative due to the sparsity of data in time and space, but they portray a new dimension of information for the zonal, secondary, and convective scales that would be extremely valuable for both research and operational purposes in meteorology.

ACKNOWLEDGMENTS

We wish to express our appreciation to Professors V. E. Suomi and L. H. Horn of the University of Wisconsin for their encouragement in the preparation of this paper. We gratefully acknowledge the assistance of Messrs. Charles Hutchins, David Barber, Mark Lipschutz, and Miss Susan Koebel in the preparation of the data and drafting and of Dr. Peter M. Kuhn in making available the radiometersonde data.

This work was supported by the Environmental Science Services Administration through WBG's 25 and 52.

REFERENCES

1. L. J. Allison, T. I. Gray, Jr., and G. Warnecke, "A Quasi-Global Presentation of TIROS III Radiation Data," *NASA SP-53*, Goddard Space Flight Center, National Aeronautics and Space Administration, Greenbelt, Md., 1964, 23 pp.
2. E. G. Astling and L. H. Horn, "Some Geographical Variations of Terrestrial Radiation Measured by TIROS II," *Journal of the Atomsopheric Sciences*, vol. 21, No. 1, Jan. 1964, pp. 30–34.
3. G. L. Darkow, "A Study of Infrared Measurements in the Vicinity of the Subtropical Tropopause," Ph. D. thesis, Department of Meteorology, University of Wisconsin, Madison, 1963.
4. J. A. Dutton and D. R. Johnson, "The Theory of Available Potential Energy and a Variation Approach to Atmospheric Energetics," *Advances in Geophysics*, vol. 12, 1967, pp. 333–436.
5. A. Eliassen, "On the Vertical Circulation in Frontal Zones," *Geofysiske Publikasjoner*, Oslo, vol. 24, 1962, pp. 147–160.
6. P. M. Kuhn and D. R. Johnson, "Improved Radiometersonde Observations of Atmospheric Infrared Irradiance," *Journal of Geophysical Research*, vol. 71, No. 2, Jan. 1966, pp. 367–373.
7. P. M. Kuhn and V. E. Suomi, "Infrared Radiometer Soundings on a Synoptic Scale," *Journal of Geophysical Research*, vol. 65, No. 11, Nov. 1960, pp. 3669–3677.
8. P. M. Kuhn and V. E. Suomi, "Airborne Radiometer Measurements of Effects of Particulates on Terrestrial Flux," *Journal of Applied Meteorology*, vol. 4, No. 2, Apr. 1965, pp. 246–252.
9. E. N. Lorenz, "Generation of Available Potential Energy and the Intensity of the General Circulation," *Dynamics of Climate*, Pergamon Press, Oxford, 1960, pp. 86–92.
10. Y. Mintz, "On the Kinematics and Thermodynamics of General Circulation of the Atmosphere in the Higher Latitudes," *Transactions of the American Geophysical Union*, vol. 28, No. 4, Aug. 1947, pp. 539–544.
11. F. Möller, "Long Wave Radiation," *Compendium of Meteorology*, American Meteorological Society, Boston, 1951, pp. 34–49.
12. V. J. Oliver, R. K. Anderson, and E. W. Ferguson, "Some Examples of the Detection of Jet Streams From TIROS Photographs," *Monthly Weather Review*, vol. 92, No. 10, Oct. 1964, pp. 441–448.
13. E. R. Reiter, *Jet-Stream Meteorology*, University of Chicago Press, 1963, 515 pp.
14. Staff Members, *TIROS II Radiation Data User's Manual*, Goddard Space Flight Center, Greenbelt, Md., 1961, 57 pp.
15. L. F. Whitney, Jr., A. Timchalk, and T. I. Gray, Jr., "On Locating Jet Streams From TIROS Photographs," *Monthly Weather Review*, vol. 94, No. 3, Mar. 1966, pp. 127–138.
16. J. S. Winston, "Zonal and Meridional Analysis of 5-Day Averaged Outgoing Long-Wave Radiation Data From TIROS IV Over the Pacific Sector in Relation to the Northern Hemisphere Circulation," *Journal of Applied Meteorology*, vol. 6, No. 3, June 1967, pp. 453–463.
17. J. S. Winston and P. K. Rao, "Preliminary Study of Planetary-Scale Outgoing Long-Wave Radiation as Derived From TIROS II Measurements," *Monthly Weather Review*, vol. 90, No. 8, Aug. 1962, pp. 307–310.

[*Received October 16, 1967; revised March 18, 1968*]